CHAPTER 2

Introduction to transiting exoplanets

The notion that Earth is a planet was not always obvious, and Earth long possessed a unique position as the centre of the universe. With the discovery of other planets in our Solar System and the realisation that the Earth revolves around the Sun, Earth's position was put into perspective, and was no longer unique, nor the centre. Even though there there were speculations about potential life beyond Earth, it took millennia before these ideas – for example advocated by Epicurus (341–270 B.C.) – could be tested (Crowe, 1999). The number of known planets was constant for a long time, before it rose again rapidly with the discovery of planets around other stars.

The detection of the first exoplanets was almost two decades ago (Wolszczan & Frail, 1992; Mayor & Queloz, 1995) and instigated a whole new field of research. However, the first detections were not planets that scientists anticipated to find, and bear little resemblance to Solar System planets. The planets found by Wolszczan & Frail (1992) were orbiting a millisecond-pulsar from which the timing could be detected using radio telescopes. While a suitable technique for detection, a millisecond-pulsar host star is not an obvious planet-hosting candidate considering the violent history these stars have gone through. Mayor & Queloz (1995) determined the radial velocity of stars by measuring Doppler line-shift using a spectrograph, and found a planet of at least half a Jupiter mass orbiting at 0.05 AU, or a period of 4 days. The authors suspect that the companion might be a very-

low-mass brown dwarf stripped of its outer atmosphere. Such a close-in massive planet provides a strong radial velocity signal, but again has no comparison in our Solar System.

With the advent of instruments such as HARPS (Mayor et al., 2003), CoRoT (Baglin et al., 2006) and Kepler (Koch et al., 1998), many planets have since been detected, and with future instruments, many more will be discovered. At the time of writing, two decades after the first detection, there are around a thousand known exoplanets, with thousands of candidates to be confirmed (see Fig. 2.1 for an overview). Most of these planets are big, massive and in close-in orbits, because detection of exoplanets is strongly affected by observation bias, but Earth-sized planets are now also within the detection range (Borucki et al., 2013).

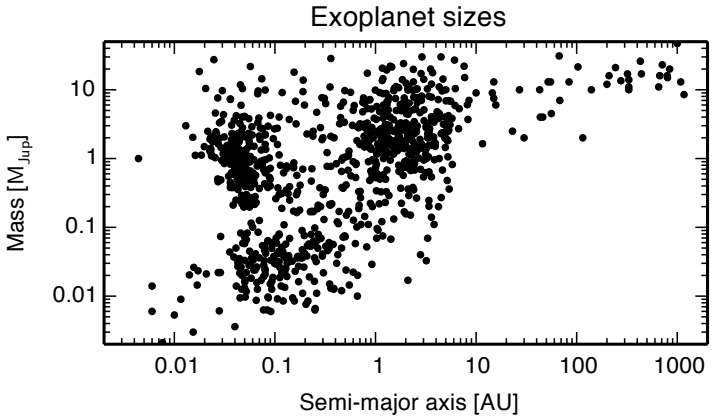

Figure 2.1: Exoplanets discovered to date, plotted as semi-major axis in against planet mass, both on logarithmic scale. Although distribution of planets in this graph are influenced by various observation biases, this plot does show the broad variety of exoplanets that exist, many having no equal in the Solar System. Data from `exoplanet.eu` (January 2014).

2.1 Detection methods

The reason that exoplanets for a long time remained undiscovered is because of the technical difficulty detecting them and because of the peculiarity of the planets detected so far, such as the objects described in the previous section. Compared to the host star, exoplanets are faint, with

Table 2.1: Number of detected exoplanets as of January 2014 grouped by detection method. Source: `exoplanet.eu`.

Method	Planet systems	Planets
Radial velocity	411	548
Transit	329	435
Imaging	43	47
Microlensing	24	26
Timing	13	16
Total	810	1074

a brightness contrast of up to nine orders of magnitude for the case of Jupiter, or ten order of magnitude for Earth for visible light (Des Marais et al., 2002). In addition, exoplanets appear in close proximity to their bright host, making it even more difficult to observe these bodies directly as the telescope's point spread function smears out the starlight (Oppenheimer & Hinkley, 2009). These values are strongly dependent on wavelength, and choosing this carefully helps significantly in reducing the contrast requirements. However, using techniques such as adaptive optics, coronagraphy, polarimetry, angular differential imaging, etc., this has now been achieved for tens of systems (Oppenheimer & Hinkley, 2009). The first directly imaged exoplanets were under less demanding circumstances, with relatively dim host stars and hot, large, wide-orbiting planets. These circumstances lower the required contrast mentioned before when observing in the infrared; the hot, large planet is intrinsically brighter, the parent star is fainter and the large separation between planet and host star is less demanding on the spatial resolution. Indeed the first direct detection was a roughly 4 Jupiter-mass planet orbiting at 46 AU from its host brown dwarf (Chauvin et al., 2005), and subsequent early detections were under similar circumstances (Marois et al., 2008; Kalas et al., 2008). With the upcoming 40-meter class telescopes and extreme-AO enabled instruments (e.g. GPI (Macintosh et al., 2008), SPHERE (Beuzit et al., 2008)), the observable part of the relevant phase-space will expand, uncovering more planets. In spite of this progress, it is technically less challenging to indirectly detect planets, for example by radial velocity, microlensing, pulsar timing, or by transit surveys Struve (1952). An overview of detected planet systems grouped by method is given in Table 2.1.

2.2 Transit analysis

One technique suitable for routine detection of exoplanets is by monitoring the brightness of stars. In the rare geometrical configuration that an exoplanet passes in between us and its host star, it can be detected as a temporary dimming in brightness of the star. The chance that a randomly oriented circular planetary orbit geometry produces an observable transit is given by (Sackett, 1999):

$$P_{\mathrm{geom}} = 0.0045 \left(\frac{1\,\mathrm{AU}}{a} \right) \left(\frac{R_\star + R_{\mathrm{pl}}}{\mathrm{R}_\odot} \right) \tag{2.1}$$

with a the semi-major axis, $R_\star + R_{\mathrm{pl}}$ the sum of the stellar and planetary radius and $\mathrm{R}_\odot$ the solar radius. To put this into perspective, for an observer looking at the Sun from a random, distant location, there is a 1 in 200 chance that he or she can observe Earth transit the Sun, and only a 1 in 1000 chance to see Jupiter transit. On the other hand, a planet in an orbit with an 0.03 AU semi-major axis has a geometrical detection probability of roughly 15 per cent, and indeed such close-in planets have been detected abundantly (see Fig. 2.1). In the case that an exoplanet is indeed in such a transiting geometry, the maximum amount of fractional dimming for a non-limb darkened star is equal the ratio of the planet to stellar surface (Sackett, 1999), i.e.

$$\Delta F \approx \left(\frac{R_{\mathrm{pl}}}{R_\star} \right)^2 . \tag{2.2}$$

To confirm that the stellar dimming was not spurious, two or three orbital periods should be observed, i.e. one can only detect planets in transits that have orbital periods a factor two or three less than the observing time, thus favouring close-in planets. Nevertheless, if one observes many stars for a long enough time, some will have planets oriented such that we can observe them transit their host star, and several missions are doing exactly this. The observation bias arising from these constraints therefore favors close-in orbits for large stars with large planetary-to-stellar radius ratios. On top of that, we can only confirm orbits for which the period is smaller than our observation baseline. Finally, there is a significant false-positive rate for planet detection through transit analysis on the order of tens of per cents (Brown, 2003; Collier Cameron et al., 2007) Follow up studies with, for example, radial velocity analysis are necessary to confirm detection of a planet, and not a small star, for example.

Figure 2.2 shows an example of the light curve induced by a transiting exoplanet. While this only gives the intensity as a function of time, a wealth

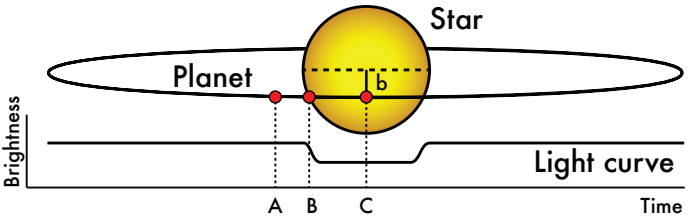

Figure 2.2: Example of a transit light curve. The points A, B and C mark the out-of-transit, ingress and mid-eclipse points, respectively, while b indicates the impact parameter (see text for details). The gradual darkening of the star towards the edge represents limb darkening. *Image credit: Wikipedia, the free encyclopedia, Nikola Smolenski*

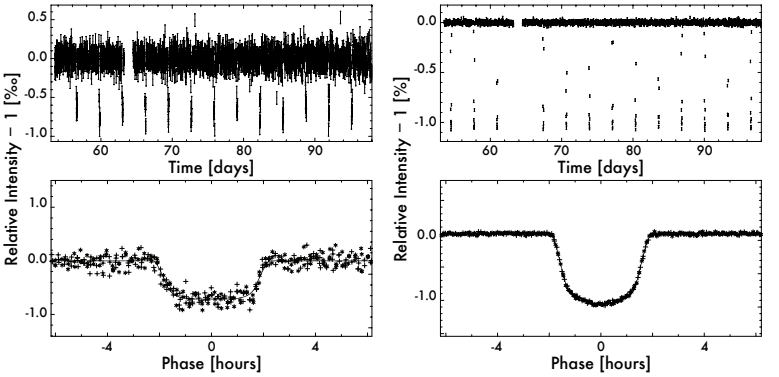

Figure 2.3: Light curves for Kepler 4b (left) and 5b (right), the first exoplanets detected uniquely by Kepler. In both panels, the top graph shows the light curve as a function of time, the bottom graph shows the curve folded with the orbital period. Kepler 4b induces an observed dimming of its host star of 0.07 per cent, and takes about 4 hours to cross the stellar disk while Kepler 5b's dimming is ten times as deep with 0.7 per cent dimming, also lasting 4 hours. Both planet's orbital period are short at 3 d. Note the different vertical scale in the different panels. *Image credit: NASA.*

of information can be extracted from the precise shape of the light curve. When multiple transits of the same object are observed, this gives the orbital period of the object, and thus the distance to the host star. The maxim depth of the eclipse (at C in Fig. 2.2) is a proxy for the eclipsed surface of the star and thus the radius of the planet, while a secondary eclipse, where the star eclipses the planet, yields the brightness of the planet. Changes in the

period can be signs of other bodies perturbing the transiting object, such as other planets. The shape of the ingress (B in Fig. 2.2) and egress gives information on the impact parameter (b in Fig. 2.2), the shape of the object, and the intensity distribution over the stellar surface, i.e. limb darkening. The shape of the minimum of the transit light curve (at C in Fig. 2.2) gives further information on the impact parameter and stellar intensity distribution. If spectra during the transit are available, the difference with the stellar spectrum can even give insight into the composition of the planetary atmosphere, without the need to resolve the planet.

Since transits only require photometry of a star, this can be used to monitor many stars at the same time. In spite of the small chance of transiting geometries, many transiting exoplanets can be detected this way. Such a survey can then be used in a statistical sense, where populations of exoplanets can be characterised. Furthermore, like radial velocity, it is a useful tool for first detection of planets, after which one can investigate the object in more detail.

2.3 Characterising exoplanets

With exoplanets detection now an almost daily routine, the next step is characterisation of the planets found. While parameters such as orbital period, mass and radius are known for many exoplanets, this still leaves room for differences between the objects. For example the Solar System's giant planets all have roughly the same radius and metallicity, but these planets are very different from one another (Oppenheimer & Hinkley, 2009).

There are exoplanets for which the atmosphere has been characterised to some extent, including HD 189733b where Swain et al. (2008) found methane. With future missions such as the Exoplanet Characterisation Observatory (EcHO), this will become more common (Tinetti et al., 2012). The exoplanets treated in this thesis are one of the few exoplanets where we can study the composition of the rocky planet itself in the case of KIC 1255b and exoplanetary rings for J1407.

Although exoplanets were peculiar objects twenty years ago, now they are discovered at rates in the hundreds per year, and we can confirm that exoplanets are indeed common. With exoplanet characterisation being the next step in this field, peculiar objects like J1407 and KIC 1255b can already provide insight into some characteristics. Transit surveys are therefore powerful tools in detecting suitable exoplanets for characterisation, and thus help develop our understanding of planets in general.

2.4 This thesis

In this thesis, we make some first steps towards exoplanet characterisation. We investigate two peculiar transiting exoplanets, *Kepler* KIC 12557548 (KIC 1255 for short) and of *SuperWASP* J140747.93−394542.6 (J1407). The former shows a 16-hour periodic transit signal with varying eclipse depth and shape from orbit to orbit, with little to no apparent correlation between consecutive orbits. This star was observed with the *Kepler* satellite While the rocky planet itself is too small to observe, it produces large amount of dust that form a cloud trailing the planet, that provides clues on the composition of the planet. The variability of the dust cloud size additionally gives insight on the dynamical processes underlying the dust generation processes. The latter was observed only once with *SuperWASP* during 2007, where the full transit lasted more than 50 days. This light curve shows a wealth of fine-structure while it is roughly symmetric around the transit epoch, consistent with the presence of a complex ring system and potentially exomoons. If this is indeed the case, J1407 is not unlike Saturn in both having complex rings and moons. The presence of a ring structure would also here provide a unique opportunity for investigation of the matter which makes up planets.

Both objects, while being different and peculiar in their own way, give a rare window of opportunity for investigation of the composition of exoplanets. The former exposes its rocky material through evaporation by the host star, the other modulates its host's light, imprinting its signature on the light curve observed by us. It is therefore likely that these planets will be the subject of much scrutiny in the coming years.

Kepler KIC 1255

For planetary transits, the geometry is often symmetrical, and this yields a symmetric transit signal, such as the transits of Kepler 4b and 5 (Fig. 2.3). Deviation from symmetry therefore indicates an asymmetry in the system, which is the case with KIC 1255. The light curve, shown in Fig. 2.4 shows a slight bump just before ingress, a steep ingress, and a gradual egress. Another curiosity of this system is the variable transit depth, ranging from less than 0.1 per cent to more than 1 per cent. The absence of some transits implies that the eclipse signal by the planet is negligible, and that the planet itself must therefore be tiny.

This target was found by Rappaport et al. (2012) and investigated by others in detail (Brogi et al., 2012; Budaj, 2013; Perez-Becker & Chiang, 2013). It appears that the close proximity to the host star of 0.013 AU (roughly 4 stel-

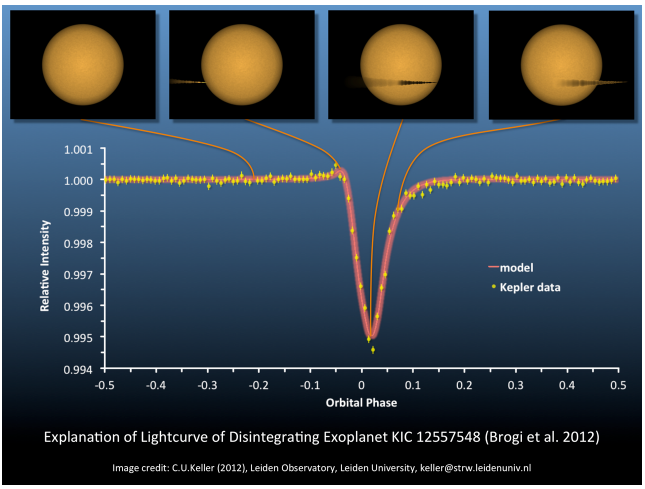

Figure 2.4: Schematic illustration of a KIC1255b model explaining the various features of the light curve.

lar radii) is causing the evaporation of the planet. The stellar flux would evaporate the rocky surface of the planet, causing a dust cloud to eclipse the star. According to this scenario, the planet mass would be slightly less than twice the mass of the Moon (0.02 Earth mass), and lose more than 0.1 Earth-mass per gigayear (Perez-Becker & Chiang, 2013), which explains the absence of some transits: the planet is tiny.

It turns out that a model of an exponential tail fits this data well (Brogi et al., 2012). The bump before ingress can be explained by forward scattering just before ingress due to the dust particles, the deep minimum is when most dust covers the stellar disk and the egress can be interpreted as a long tail of dust trailing the planet. To explain the variable transit depth, the dust evaporation must occur on timescales of less than one orbit, in this case 16 h, and that the dust generation must be highly variable, sometimes ejecting big clouds causing more than 1 per cent dimming, while at other times generating hardly any dust to account for the shallow transits. This is not unlikely considering the planet's proximity to the host star and its influence on the planet.

In Chap. 5 of this thesis, we characterise the dust cloud tail surrounding the planet in more detail, looking at the dust cloud generation and longevity. We investigate the light curve on a per-transit basis, to find correlations between consecutive transit and egress depths, evolution of the

transit depth, and differences between different transit depths. We extended the 1-D model developed in Brogi et al. (2012) to a 2-D, 2-component model, where we model the dust cloud by an opaque, spherical core and an exponentially decaying tail attached to it. Using this improved model and the available short cadence data we can investigate the dust cloud changes from transit to transit. While we note that the model we use is not a unique solution, this analysis does provide constraints for future, more thorough modelling.

SuperWASP J1407

Another peculiar object is J1407, whose observed intensity shows a long transit with maximum dimming of 95 per cent (Mamajek et al., 2012). Although the light curve is roughly symmetric, with the ingress and egress each lasting about 25 days, the fine-structure is different between the two when folding the light curve around the eclipse midpoint. While binary stars or a circumstellar disk can explain parts of the light curve, the only scenario that seems compatible with the observations is a ringed disk around a companion to J1407. Mamajek et al. (2012) proposed and investigated this hypothesis, and found that an initial 4-ring model explains the approximate shape of the light curve.

The intriguing part about this target is the myriad of fine-structure in the light curve, with large light curve gradients of up to tens of per cent per night and inflection points during individual nights, and big intra-night differences in both dimming and light curve gradient. Using a simple face-on ring model, one can compute the light curve gradient for a given orbital speed. By fitting this to the data, one can calculate the minimum speeds implied by these light curve-gradient. We performed this analysis in Chap. 6 and found minimum speeds of up to 33 $\mathrm{km\,s^{-1}}$, which are incompatible with the maximum orbital speed of 22 $\mathrm{km\,s^{-1}}$ found by Mamajek et al. (2012), even assuming optimal geometric conditions for the ring model.

Using these implied speeds from the light curve and the transit duration of 54 days, we also derived a minimum ring-disk diameter in the range of 0.05 to 0.5 AU, which is 16 to 160 times as large compared to Saturn's 480×10^3 km outer E-ring radius. Furthermore, the maximum semi-major axis for a circular orbit would be between 0.8 to 10 AU.

Since these speeds are incompatible with the constraints presented by Mamajek et al. (2012), this simple model fails to explain the data. One possible solution to this problem could be azimuthal structure in the ring, such as the 'spokes' observed in Saturn's B-rings (Smith et al., 1982). Un-

der favourable orientations, the rotational speed of such spokes could add to the planet speed to account for the observed light curve gradients. Although a possible explanation, it is not clear whether this is indeed the case, as it requires a careful and unlikely alignment of the disk and spokes to match the observations.